

# Giant-Atom Effects on Population and Entanglement Dynamics of Rydberg Atoms

Yao-Tong Chen,<sup>1</sup> Lei Du,<sup>1,\*</sup> Yan Zhang,<sup>1</sup> Lingzhen Guo,<sup>2</sup> Jin-Hui Wu,<sup>1,†</sup> M. Artoni,<sup>3,4</sup> and G. C. La Rocca<sup>5</sup>

<sup>1</sup>*School of Physics and Center for Quantum Sciences,  
Northeast Normal University, Changchun 130024, China*

<sup>2</sup>*Center for Joint Quantum Studies and Department of Physics,  
School of Science, Tianjin University, Tianjin 300072, China*

<sup>3</sup>*Department of Chemistry and Physics of Materials, University of Brescia, Italy*

<sup>4</sup>*European Laboratory for Non-Linear Spectroscopy, Sesto Fiorentino, Italy*

<sup>5</sup>*NEST, Scuola Normale Superiore, Piazza dei Cavalieri 7, I-56126 Pisa, Italy*

(Dated: May 1, 2023)

Giant atoms are attracting interest as an emerging paradigm in the quantum optics of engineered waveguides. Here we propose to realize a synthetic giant atom working in the optical regime starting from a pair of interacting Rydberg atoms driven by a coherent field and coupled to a photonic crystal waveguide. Giant-atom effects can be observed as a phase-dependent decay of the double Rydberg excitation during the initial evolution of this atomic pair while (internal) atomic entanglement is exhibited at later times. Such an intriguing entanglement onset occurs in the presence of intrinsic atomic decay toward non-guided vacuum modes and is accompanied by an anti-bunching correlation of the emitted photons. Our findings may be relevant to quantum information processing, besides broadening the giant-atom waveguide physics with optically driven natural atoms.

*Introduction.*—A fascinating paradigm of quantum optics dubbed “giant atom” has been developed recently to describe situations where artificial atoms interact with microwave or acoustic fields beyond the standard dipole approximation [1]. With state-of-the-art technologies, one can implement giant atoms that are coupled to a waveguide at multiple points, with coupling separations comparable to field wavelengths. These nonlocal interactions can result in peculiar self-interference effects, which account for a number of phenomena not happening in conventional natural atoms, such as frequency-dependent atomic relaxation rates and Lamb shifts [2–6], non-exponential atomic decay [7–9], in-band decoherence-free interactions [3, 10–12], and exotic atom-photon bound states [13–18]. To date, platforms capable of implementing giant atoms mainly include superconducting quantum circuits [3, 8, 19, 20], coupled waveguide arrays [21], and cold atoms in state-dependent lattices [22], but have also been extended to synthetic frequency dimensions [23] and ferromagnetic spin systems [24].

Nevertheless, it is important to explore new physics of giant atoms within different atomic architectures, especially those working beyond the microwave or acoustic regime and with high-lying Rydberg atoms. Owing to unique properties unlike atoms in the ground or low-lying excited states, including strong dipole-dipole interactions and long radiative lifetimes [25], Rydberg atoms turn out to be an excellent building block in quantum information processing, with potential applications for realizing quantum logic gates [26–29], single-photon sources [30–33], and various entangled states [34–37]. Rydberg atoms have also been successfully employed in waveguide quantum electrodynamics by coupled to engineered structures like optical nanofibers [38], photonic crystal waveguides [39], and coplanar microwave waveguides [40].

In this Letter, we consider a pair of two-level Rydberg atoms coupled to a photonic crystal waveguide (PCW) through two lower transitions and driven by a coherent field through two upper transitions in the two-atom basis to display giant-atom effects in the optical regime. The self-interference effect appears specifically at *shorter times* of the pair’s dynamic evolution dominated by two competing two-photon resonant transitions, thereby realizing a *synthetic* giant atom with two coupling points at a variable distance  $d$  about the atomic separation  $R$ . For *longer times*, on the other hand, we observe the onset of atomic entanglement through mutual Rydberg excitations of the two atoms as the phase  $\phi$  accumulated from a coupling point to the other takes specific values, which depends on  $d$  and is tunable. This effect is characterized by a detailed examination on *quantum correlations* of the emitted photons and further understood in terms of *dark states* decoupled from both coherent field and waveguide modes. Our findings remain valid even for continuous atom-waveguide couplings, which are more appropriate for Rydberg atoms with large spatial extents.

*Model.*—We start by illustrating in Fig. 1(a) that a pair of Rydberg atoms with ground  $|g_{1,2}\rangle$  and Rydberg  $|r_{1,2}\rangle$  states separated by frequency  $\omega_e$  are trapped in the vicinity of a PCW [41, 42] at  $x_1 = 0$  and  $x_2 = d$ , respectively. The two atoms are illuminated by a coherent field of frequency  $\omega_c$  and interact through a (repulsive) van der Waals (vdW) potential  $V_6 = C_6/R^6$ , when *both* excited to the Rydberg states, with  $C_6$  being the vdW coefficient and  $R$  the interatomic distance, which could be different from  $d$  [43]. The vdW interaction will result in a largely shifted energy  $2\hbar\omega_e + \hbar V_6$  for the *double-excitation* state  $|r_1 r_2\rangle$  while the *single-excitation* states  $|r_1 g_2\rangle$  and  $|g_1 r_2\rangle$  remain to exhibit energy  $\hbar\omega_e$ . In the two-atom basis, for a large enough  $V_6$ , we have the four-level configuration

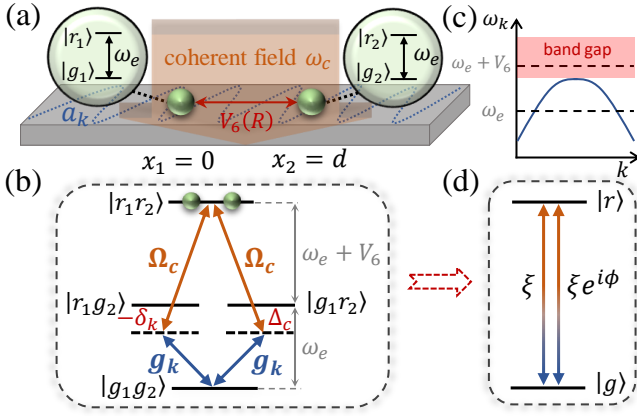


FIG. 1. (a) The two-level configuration (*single-atom basis*). Two Rydberg atoms placed at a distance  $R$  interact via a potential  $V_6(R)$  and couple to a waveguide mode  $a_k$  at  $x_1 = 0$  or  $x_2 = d$  while driven by a coherent field  $\omega_c$ . (b) The four-level configuration (*two-atom basis*). Blue (red) lines represent single (double) Rydberg excitations, whereby two lower (upper) transitions are coupled by mode  $a_k$  of strength  $g_k$  (field  $\omega_c$  of strength  $\Omega_c$ ). (c) The dispersion relation of a PCW: frequency  $\omega_e$  of the lower transitions falls within the propagating band while frequency  $\omega_e + V_6$  of the upper transitions falls within the band gap (red shaded). (d) An equivalent two-level giant atom with  $|g\rangle \equiv |g_1g_2\rangle$  and  $|r\rangle \equiv |r_1r_2\rangle$ , upon adiabatic elimination of the single-excitation states, bears separate couplings of strengths  $\xi$  at  $x_1$  and  $\xi e^{i\phi}$  at  $x_2$ , with  $\phi$  being the accumulated phase between  $x_1$  and  $x_2$ .

shown in Fig. 1(b) whereby the coherent field  $\omega_c$  drives only transitions  $|g_1r_2\rangle \leftrightarrow |r_1r_2\rangle$  and  $|r_1g_2\rangle \leftrightarrow |r_1r_2\rangle$  with detuning  $\Delta_c = \omega_c - (\omega_e + V_6)$  and strength  $\Omega_c$ , while a waveguide mode of frequency  $\omega_k$  (wavevector  $k$ ) drives only transitions  $|g_1g_2\rangle \leftrightarrow |g_1r_2\rangle$  and  $|g_1g_2\rangle \leftrightarrow |r_1g_2\rangle$  with detuning  $\delta_k = \omega_k - \omega_e$  and strength  $g_k$ . This scheme is supported by the following two considerations. *First*,  $\omega_c$  is far away from  $\omega_e$  but close to  $\omega_e + V_6$  with  $\Delta_c \ll V_6$ , so that the coherent field can only drive two upper transitions. *Second*,  $\omega_e$  and  $\omega_e + V_6$  fall, respectively, within the lower propagating band and the band gap of a PCW as sketched in Fig. 1(c), so that the waveguide mode can only drive two lower transitions.

Then, for a continuum of waveguide modes interacting only with two lower transitions, the Hamiltonian in the rotating-wave approximation is ( $\hbar = 1$ )

$$\begin{aligned}
 H = & \omega_e(\sigma_+^1\sigma_-^1 + \sigma_+^2\sigma_-^2) + (\omega_e + V_6/2)(\sigma_+^3\sigma_-^3 + \sigma_+^4\sigma_-^4) \\
 & + \int dk \omega_k a_k^\dagger a_k + \left[ \int dk g a_k (\sigma_+^1 + e^{ikd}\sigma_+^2) \right. \\
 & \left. + \Omega_c e^{-i\omega_c t} (\sigma_+^3 + \sigma_+^4) + \text{H.c.} \right].
 \end{aligned} \tag{1}$$

Here, we have introduced the atomic raising operators  $\sigma_+^1 = |r_1g_2\rangle\langle g_1g_2|$ ,  $\sigma_+^2 = |g_1r_2\rangle\langle g_1g_2|$ ,  $\sigma_+^3 = |r_1r_2\rangle\langle r_1g_2|$ , and  $\sigma_+^4 = |r_1r_2\rangle\langle g_1r_2|$  (two-atom basis) while the corre-

sponding lowering operators are  $\sigma_-^j = (\sigma_+^j)^\dagger$ . Moreover,  $a_k^\dagger$  and  $a_k$  refer, respectively, to the creation and annihilation operators of a waveguide mode  $\omega_k$ . We have also assumed constant coupling strengths, i.e.  $g_k \simeq g$ , in the Weisskopf-Wigner approximation.

As we address only the two-atom dynamics, the waveguide modes of density  $D(k)$  at frequency  $\omega_k$  can be traced out (Born-Markov approximation), yielding the master equation for density operator  $\rho$  [43, 46, 47]

$$\begin{aligned}
 \partial_t \rho = & -i[H_{at}, \rho] + \sum_{i=1}^4 \gamma \mathcal{L}[\sigma_-^i] \rho + \sum_{j=1}^2 \Gamma \mathcal{L}[\sigma_-^j] \rho \\
 & + \Gamma_{ex} \left[ (\sigma_-^1 \rho \sigma_+^2 - \frac{1}{2} \{ \sigma_+^1 \sigma_-^2, \rho \}) + \text{H.c.} \right],
 \end{aligned} \tag{2}$$

where  $\mathcal{L}[O]\rho = O\rho O^\dagger - \frac{1}{2}\{O^\dagger O, \rho\}$  is the Lindblad superoperator describing two-atom decay processes, with  $\Gamma(k) = 4\pi g^2 D(k)$  denoting the decay rate into relevant modes of the waveguide (guided modes) [2, 3] while  $\gamma$  being the mean decay rate into other electromagnetic modes (non-guided modes). Under the two-photon resonance condition  $\Delta_c + \delta_k \simeq 0$ , assumed to hold for all guided modes, the atomic Hamiltonian is

$$\begin{aligned}
 H_{at} = & \Delta_c(\sigma_+^1\sigma_-^1 + \sigma_+^2\sigma_-^2) + J_{ex}(\sigma_+^1\sigma_-^2 + \sigma_+^2\sigma_-^1)/2 \\
 & + [\Omega_c(\sigma_+^3 + \sigma_+^4) + \text{H.c.}],
 \end{aligned} \tag{3}$$

with  $J_{ex} = \Gamma \sin\phi$  and  $\Gamma_{ex} = \Gamma \cos\phi$  denoting, respectively, *coherent* and *dissipative* parts of the exchange interaction mediated by the waveguide. Here we have defined  $\phi(k) = |k|d = \omega_k d / |v_g(k)| \simeq \omega_e d / |v_g(k)|$  with  $v_g(k)$  being the group velocity of a guided mode bearing the “linearized” dispersion  $\omega_k \simeq kv_g(k)$ . It is worth stressing that  $\Gamma_{ex}$  serves as a reservoir to *engineer* the atomic decay through selected guided modes  $\omega_k$  (or bandwidth of modes) and their density distribution  $D(k)$ . In turn, such an engineered reservoir together with the atomic separation  $d$  represents a set of knobs to control the phase  $\phi(k)$  acquired by an emitted photon between the *contact points*  $x_1$  and  $x_2$  of a giant-atom (see below).

*Synthetic two-level giant atom: the short-time regime.*— Maintaining  $\Delta_c + \delta_k \simeq 0$  and further requiring  $|\Delta_c| \gg \Omega_c, g$ , the two atoms initially in the double Rydberg state  $|r_1r_2\rangle$  would behave like a two-level giant atom decaying directly to the ground state  $|g_1g_2\rangle$  at two coupling points  $x_1$  and  $x_2$ . This expectation will be verified by numerically comparing the dynamics of the four-level atomic pair to that of the synthetic two-level giant atom. In the latter picture, the two atoms interact with the waveguide modes only through the two-photon resonant transition  $|r_1r_2\rangle \leftrightarrow |g_1g_2\rangle$  whereby an external photon of frequency  $\omega_c$  and a waveguide photon of frequency  $\omega_k$  are emitted (or absorbed) at the same time. Upon the adiabatic elimination of states  $|r_1g_2\rangle$  and  $|g_1r_2\rangle$  [48, 49], the effective

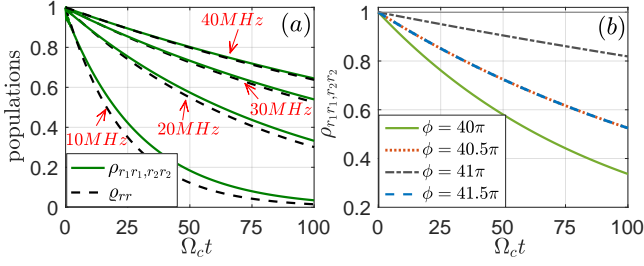


FIG. 2. (a) Time evolutions of double Rydberg population  $\rho_{r_1 r_1, r_2 r_2}$  and giant-atom population  $\varrho_{rr}$  with  $\phi = 40.5\pi$  and different values of  $\Delta_c$ . (b) Time evolutions of  $\rho_{r_1 r_1, r_2 r_2}$  with  $\Delta_c = 30$  MHz and different values of  $\phi$ . Other parameters are  $V_6 = 20$  GHz,  $\Omega_c = 1.0$  MHz,  $\Gamma = 1.0$  MHz, and  $\gamma = 1.0$  kHz. The thin gray line in (b) is shown as a reference for  $\gamma = 0$  (no intrinsic decay) with  $\Delta_c = 30$  MHz and  $\phi = 41\pi$ .

$|r_1 r_2\rangle \leftrightarrow |g_1 g_2\rangle$  transition amplitude consists of two contributions:  $\xi_1 = -g\Omega_c/\Delta_c \equiv \xi$  (interaction at  $x_1 = 0$ ) and  $\xi_2 = \xi e^{i\phi}$  (interaction at  $x_2 = d$ ), as sketched in Fig. 1(d), which interfere with each other.

With the above assumptions, we write down the synthetic two-level giant-atom Hamiltonian as

$$\mathcal{H} = (2\omega_e + V_6)\sigma_+\sigma_- + \int dk(\omega_k + \omega_c)a_k^\dagger a_k + \int dk[\xi a_k(1 + e^{ikd})\sigma_+ + \text{H.c.}], \quad (4)$$

in terms of the transition operator  $\sigma_+ = (\sigma_-)^\dagger = |r\rangle\langle g|$  with  $|r\rangle \equiv |r_1 r_2\rangle$  and  $|g\rangle \equiv |g_1 g_2\rangle$ . Again, by tracing out the waveguide modes, we arrive at the master equation for giant-atom density operator  $\varrho$  [43]

$$\partial_t \varrho = 2\gamma \mathcal{L}[\sigma_-]\varrho + (\Upsilon + \Upsilon^*)\sigma_- \varrho \sigma_+ - \Upsilon \sigma_+ \sigma_- \varrho - \Upsilon^* \varrho \sigma_+ \sigma_-, \quad (5)$$

where  $\Upsilon = 4\pi\xi^2 D(1 + e^{i\phi}) = (\Gamma + \Gamma_{ex} + iJ_{ex})\Omega_c^2/\Delta_c^2$  with its real and imaginary parts being, respectively, the phase-dependent decay rate and Lamb shift.

In the remaining part, we perform numerical analysis in support of the predictions anticipated above. We first consider that for large enough (driving) detunings  $|\Delta_c|$ , the adiabatic elimination of two single-excitation states can be actually made, providing in turn an adequate evidence of the equivalence between the (four-level) atomic pair and the (two-level) giant atom in the short-time regime. This has been examined in Fig. 2(a) by comparing time evolutions of atomic-pair population  $\rho_{r_1 r_1, r_2 r_2}$  based on Eq. (2) and giant-atom population  $\varrho_{rr}$  based on Eq. (5) with matched parameters. Taking  $\phi = 40.5\pi$  as an example and starting from  $\rho_{r_1 r_1, r_2 r_2}(0) = \varrho_{rr}(0) = 1$ , we find that  $\rho_{r_1 r_1, r_2 r_2}(t)$  and  $\varrho_{rr}(t)$  exhibit a better agreement for a larger  $|\Delta_c|$  so that the adiabatic elimination leading to a giant atom becomes reliable for  $|\Delta_c|/\Omega_c \gtrsim 30$ . It is also worth noting that  $\rho_{r_1 r_1, r_2 r_2}(t)$  and  $\varrho_{rr}(t)$  decay faster as  $|\Delta_c|$  decreases because a smaller  $|\Delta_c|$  results

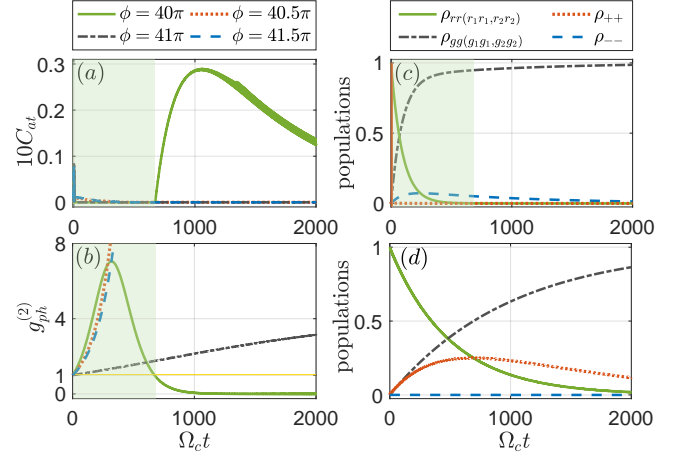


FIG. 3. Time evolutions of atomic concurrence  $C_{at}$  (a) and photonic correlation  $g_{ph}^{(2)}$  for different values of  $\phi$  (b) as well as atomic populations  $\rho_{gg}$ ,  $\rho_{rr}$ ,  $\rho_{++}$ , and  $\rho_{--}$  for  $\phi = 40\pi$  (c) and  $\phi = 41\pi$  (d) with other parameters same as in Fig. 2(b).

in a stronger coupling strength  $\xi$  and thereby a larger decay rate  $\text{Re}(\Upsilon)$  of the synthetic giant atom.

The giant-atom self-interference effect can instead be established by plotting  $\rho_{r_1 r_1, r_2 r_2}(t)$  in Fig. 2(b) for  $\Delta_c = 30$  MHz and different values of  $\phi$ . It is clear that an enhanced (reduced) decay occurs for  $\rho_{r_1 r_1, r_2 r_2}(t)$  in the case of  $\phi = 2m\pi$  ( $\phi = 2m\pi + \pi$ ) with  $m \in \mathbb{Z}$  due to a perfect constructive (destructive) interference between two coupling points, as can be seen from  $\text{Im}(\Upsilon) = 0$  and  $\text{Re}(\Upsilon) = \Gamma(1 + \cos \phi)\Omega_c^2/\Delta_c^2$ . The atomic pair is found in particular to show an undamped double-excitation population [ $\rho_{r_1 r_1, r_2 r_2}(t) \equiv 1$ ] for  $\phi = 2m\pi + \pi$  and  $\gamma = 0$ , which is one of the most remarkable features of giant atoms [2] due to a complete decoupling from the waveguide ( $\Upsilon = 0$ ) and a vanishing intrinsic decay ( $\gamma = 0$ ). In the case of  $\phi = 2m\pi \pm \pi/2$ , we have  $\text{Im}(\Upsilon) = \pm\Gamma\Omega_c^2/\Delta_c^2$  and  $\text{Re}(\Upsilon) = \Gamma\Omega_c^2/\Delta_c^2$ , which accounts for the identical population dynamics with a moderate decay since opposite detunings (Lamb shifts) make no difference.

We finally detail how one can actually adjust phase  $\phi$  while leaving potential  $V_6$  unchanged. To this end, a pair of  $^{87}\text{Rb}$  atoms with ground state  $|g_{1,2}\rangle = |5S_{1/2}, F = 2, m_F = 2\rangle$  and Rydberg state  $|r_{1,2}\rangle = |75P_{3/2}, m_J = 3/2\rangle$  of transition frequency  $\omega_e \simeq 2\pi \times 1009$  THz are taken here as an example. In this case, we have  $\gamma \simeq 1.0$  kHz for the intrinsic Rydberg lifetime  $\tau \simeq 964$   $\mu\text{s}$  while  $V_6 \simeq 20$  GHz for  $R \simeq 3.1$   $\mu\text{m}$  and  $C_6 \simeq 2\pi \times 2.8 \times 10^{12}$   $\text{s}^{-1}\mu\text{m}^6$  [50, 51]. When the atomic pair is placed exactly along the waveguide, we have  $d = R$  and hence  $\phi \simeq 41.6\pi$  by assuming that  $v_g$  is a half of the vacuum light speed  $c$ . When the atomic pair is misaligned along the waveguide, however, it is viable to attain  $d \simeq 2.95$   $\mu\text{m}$  and hence  $\phi \simeq 39.6\pi$  with neither  $R$  nor  $V_6$  changed [43].

*Atomic entanglement onset: the long-time regime.*— Now leaving the short-time regime where the atomic pair

can be modeled as a giant atom according to Eq. (5), we turn to the long-time regime where the decay toward non-guided vacuum modes becomes important as less and less population can be found in the double-excitation state. A peculiar aspect of the long-time regime is internal entanglement of the atomic pair (i.e., a specific superposition of two single-excitation states) generated by the coherent interaction described by  $H_{at}$ , which can be quantified by the Wootters concurrence [52–54]

$$C_{at} = \text{Max}(0, \lambda_1 - \lambda_2 - \lambda_3 - \lambda_4) \quad (6)$$

with  $\lambda_1 > \lambda_2 > \lambda_3 > \lambda_4$  being the four eigenvalues of matrix  $X$  defined by  $X^2 = \sqrt{\rho}(\sigma_y \otimes \sigma_y)\rho^*(\sigma_y \otimes \sigma_y)\sqrt{\rho}$  and the standard Pauli matrix  $\sigma_y$ . This concurrence takes values in the range of  $[0, 1]$  with  $C_{at} = 0$  ( $C_{at} = 1$ ) denoting a non-entangled (maximally entangled) state and is related to the correlation function [55–57]

$$g_{ph}^{(2)} = \frac{\rho_{r_1 r_1, r_2 r_2}}{\rho_{r_1 r_1} \rho_{r_2 r_2}} \quad (7)$$

of the photons emitted by two Rydberg atoms. As usual,  $\rho_{r_1 r_1} = \langle r_1 | \text{Tr}_2 \rho | r_1 \rangle$  and  $\rho_{r_2 r_2} = \langle r_2 | \text{Tr}_1 \rho | r_2 \rangle$  are obtained from reduced density matrices of different atoms, while  $g_{ph}^{(2)} > 1$  and  $g_{ph}^{(2)} < 1$  refer to the effects of photon bunching and anti-bunching, respectively.

We plot in Fig. 3(a) time evolutions of  $C_{at}$  for different values of  $\phi$  starting from the same double-excitation state and find that  $C_{at}$  becomes suddenly nonzero at a critical time for  $\phi = 2m\pi$  but remains vanishing for other values of  $\phi$ . Such an onset of internal atomic entanglement happens when the photon correlation function  $g_{ph}^{(2)}$  evolves from the regime of bunching to that of anti-bunching as shown in Fig. 3(b). This signifies a rigid correspondence between the emergence of photon anti-bunching and the generation of atomic entanglement.

It is worth noting that  $g_{ph}^{(2)}$  also indicates how the two Rydberg atoms are distributed in the single- and double-excitation states, which would be helpful to understand the underlying physics of the entanglement sudden-onset dynamics. This inspires us to further plot  $\rho_{gg}$ ,  $\rho_{rr}$ ,  $\rho_{++}$ , and  $\rho_{--}$  in Fig. 3(c) for  $\phi = 2m\pi$  and Fig. 3(d) for  $\phi = 2m\pi + \pi$  with  $|g\rangle \equiv |g_1 g_2\rangle$ ,  $|r\rangle \equiv |r_1 r_2\rangle$ , and  $|\pm\rangle \equiv 1/\sqrt{2}(|r_1 g_2\rangle \pm |g_1 r_2\rangle)$  by considering that  $|+\rangle$  ( $|-\rangle$ ) is the symmetric (anti-symmetric) dressed state of  $H_{at}$  in the case of  $\phi = m\pi$  due to  $J_{ex} = 0$ . To be more specific, we have the following dynamic equations [43]

$$\begin{aligned} \partial_t \rho_{++} &= -\gamma_+ \rho_{++} + \gamma \rho_{rr} + i\Omega_c^* \rho_{r+} - i\Omega_c \rho_{+r}, \\ \partial_t \rho_{--} &= -\gamma_- \rho_{--} + \gamma \rho_{rr}, \end{aligned} \quad (8)$$

with  $\gamma_{\pm} = \gamma + \Gamma \pm \Gamma_{ex}$ . It is clear that  $|-\rangle$  is decoupled from field  $\Omega_c$  and will become a *dark* state if it is further immune to the waveguide modes in the case of  $\phi = 2m\pi$ . However,  $|+\rangle$  is always a *bright* state in that its dynamics depends on field  $\Omega_c$  all the time.

Note in particular that  $\gamma_+ = \gamma + 2\Gamma \gg \gamma_- = \gamma$  in the case of  $\phi = 2m\pi$ , which explains why  $\rho_{++}$  remains to be vanishing while  $\rho_{--}$  does not in Fig. 3(c) so that we have  $g_{ph}^{(2)} \simeq 4\rho_{rr}/\rho_{--}^2$ . The atomic entanglement onset occurs for  $\phi = 2m\pi$  just because a dark state immune to field  $\Omega_c$  allows the transition from  $4\rho_{rr} > \rho_{--}^2$  to  $4\rho_{rr} < \rho_{--}^2$ . In the case of  $\phi = 2m\pi + \pi$ , however, we have a nonzero  $\rho_{++}$  and a vanishing  $\rho_{--}$  in Fig. 3(d) and hence  $g_{ph}^{(2)} \simeq 4\rho_{rr}/\rho_{++}^2$  due to  $\gamma_- = \gamma + 2\Gamma \gg \gamma_+ = \gamma$ . The atomic entanglement onset is absent for  $\phi = 2m\pi + \pi$  just because a bright state interacting with field  $\Omega_c$  always results in  $4\rho_{rr} > \rho_{++}^2$ . Finally, we stress that  $\rho_{++} > 0$  ( $\rho_{--} > 0$ ) and  $\rho_{--} = 0$  ( $\rho_{++} = 0$ ) do not mean that the decomposition of a mixed state  $\rho$  must include a pure state  $|+\rangle$  ( $|-\rangle$ ), hence do not mean that we must have  $C_{at} > 0$ , which further explains why  $C_{at}$  could suddenly become nonzero only for  $\phi = 2m\pi$ .

*Continuous couplings.*—Working with point-like atom-waveguide couplings, as assumed so far, is just a rough approximation for highly-excited Rydberg states of size  $\bar{r} \propto n^2$ , with  $n$  being the principal quantum number. We then extend our discrete-coupling configuration results to the continuum limit whereby the coupling region becomes a large ensemble of coupling points, each with a different strength. For an exponential continuous distribution [8] of such coupling strengths as in Fig. 4(a) spread about each contact point with a characteristic width  $\Theta$ , we find that the master equations (2) and (5) can be generalized to the continuous-coupling limit by replacing  $\Gamma \rightarrow \Gamma'$ ,  $\Gamma_{ex} \rightarrow \Gamma'_{ex}$ ,  $J_{ex} \rightarrow J'_{ex}$  and  $\Upsilon \rightarrow \Upsilon'$  while simultaneously introducing an interaction term  $J'(\sigma_+^1 \sigma_-^1 + \sigma_+^2 \sigma_-^2)$  in Eq. (3). While explicit expressions of these modified parameters are given in [43], we here use them to plot in Figs. 4(b) and 4(c) the time evolutions of  $\rho_{r_1 r_1, r_2 r_2}$  and  $C_{at}$  in the short-time and long-time regimes, respectively, for different values of  $\phi$  and a fixed  $\Theta$ .

It is easy to see that the giant-atom effects of phase-dependent population decay and entanglement onset remain observable for a remarkable coupling broadening. Moreover, the dynamic behavior of  $\rho_{r_1 r_1, r_2 r_2}$  for  $\Theta = 5\pi/2$  (continuous couplings) is identical to that for  $\Theta = 0$  (point-like couplings) in the case of  $\phi = 2m\pi + \pi$  since there is no decay toward the waveguide with  $\text{Re}(\Upsilon') = 0$ . Note, however, that a nonzero Lamb shift with  $\text{Im}(\Upsilon') \neq 0$  always exists for continuous couplings [43], which does not affect atomic population decay but would be relevant to other problems such as photon scattering.

*Conclusions.*—We have proposed a feasible scheme for constructing a synthetic giant atom with two interacting Rydberg atoms coupled to a PCW and driven by a coherent field. Giant-atom effects are manifested by a phase-dependent population dynamics in the short-time regime and an entanglement sudden-onset dynamics in the long-time regime. These effects are observable even for continuous atom-waveguide couplings, indicating their robust-

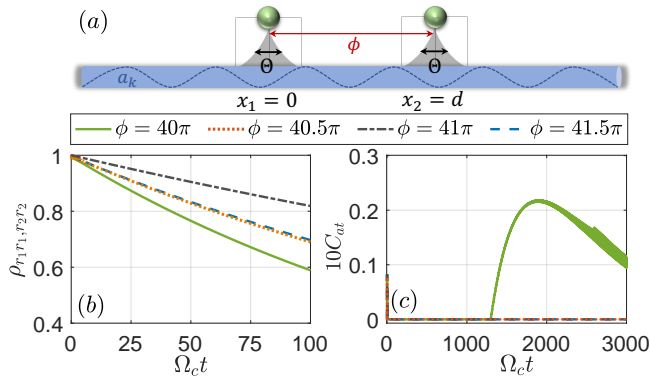


FIG. 4. (a) Schematic of two Rydberg atoms close to a waveguide with identical exponential coupling distributions around  $x_1 = 0$  and  $x_2 = d$ . Time evolutions of population  $\rho_{r_1 r_1, r_2 r_2}$  (b) and concurrence  $C_{at}$  (c) with  $\Theta = 5\pi/2$  and different values of  $\phi$ . Other parameters are the same as in Fig. 2(b).

ness against the unavoidable coupling broadening. Compared to typical schemes utilizing superconducting quantum circuits, our Rydberg scheme provides a promising platform for studying giant-atom physics in the optical regime. Hence, our findings have potential applications in quantum network engineering and quantum information processing based on optical photons.

This work is supported by the National Natural Science Foundation of China (No. 12074061), the National Key Research and Development Program of China (No. 2021YFE0193500), and the Italian PNRR MUR (project PE0000023-NQSTI).

\* [dul256@nenu.edu.cn](mailto:dul256@nenu.edu.cn)

† [jhwu@nenu.edu.cn](mailto:jhwu@nenu.edu.cn)

## REFERENCES

- [1] A. F. Kockum, [Quantum optics with giant atoms—the first five years](#), p125-p146 in *Mathematics for Industry* (Springer Singapore, 2021).
- [2] A. F. Kockum, P. Delsing, and G. Johansson, Designing frequency-dependent relaxation rates and Lamb shifts for a giant artificial atom, *Phys. Rev. A* **90**, 013837 (2014).
- [3] B. Kannan, M. Ruckriegel, D. Campbell, A. F. Kockum, J. Braumüller, D. Kim, M. Kjaergaard, P. Krantz, A. Melville, B. M. Niedzielski, A. Vepsäläinen, R. Winik, J. Yoder, F. Nori, T. P. Orlando, S. Gustavsson, and W. D. Oliver, Waveguide quantum electrodynamics with superconducting artificial giant atoms, *Nature (London)* **583**, 775 (2020).
- [4] Q. Y. Cai and W. Z. Jia, Coherent single-photon scattering spectra for a giant-atom waveguide-QED system beyond the dipole approximation, *Phys. Rev. A* **104**, 033710 (2021).
- [5] Y. T. Chen, L. Du, L. Guo, Z. Wang, Y. Zhang, Y. Li, and J. H. Wu, Nonreciprocal and chiral single-photon scattering for giant atoms, *Commun. Phys.* **5**, 215 (2022).
- [6] X.-L. Yin, Y.-H. Liu, J.-F. Huang, and J.-Q. Liao, Single-photon scattering in a giant-molecule waveguide-QED system, *Phys. Rev. A* **106**, 013715 (2022).
- [7] L. Guo, A. L. Grimsmo, A. F. Kockum, M. Pletyukhov, and G. Johansson, Giant acoustic atom: A single quantum system with a deterministic time delay, *Phys. Rev. A* **95**, 053821 (2017).
- [8] G. Andersson, B. Suri, L. Guo, T. Aref, and P. Delsing, Nonexponential decay of a giant artificial atom, *Nat. Phys.* **15**, 1123 (2019).
- [9] Q.-Y. Qiu, Y. Wu, and X.-Y. Lü, Collective Radiance of Giant Atoms in Non-Markovian Regime, *Sci. China Phys. Mech. Astron.* **66**, 224212 (2023).
- [10] A. F. Kockum, G. Johansson, and F. Nori, Decoherence-Free Interaction between Giant Atoms in Waveguide Quantum Electrodynamics, *Phys. Rev. Lett.* **120**, 140404 (2018).
- [11] A. Carollo, D. Cilluffo, and F. Ciccarello, Mechanism of decoherence-free coupling between giant atoms, *Phys. Rev. Research* **2**, 043184 (2020).
- [12] A. Soro, and A. F. Kockum, Chiral quantum optics with giant atoms, *Phys. Rev. A* **105**, 023712 (2022).
- [13] L. Guo, A. F. Kockum, F. Marquardt, and G. Johansson, Oscillating bound states for a giant atom, *Phys. Rev. Research* **2**, 043014 (2020).
- [14] X. Wang, T. Liu, A. F. Kockum, H.-R. Li, and F. Nori, Tunable Chiral Bound States with Giant Atoms, *Phys. Rev. Lett.* **126**, 043602 (2021).
- [15] W. Zhao and Z. Wang, Single-photon scattering and bound states in an atom-waveguide system with two or multiple coupling points, *Phys. Rev. A* **101**, 053855 (2020).
- [16] H. Xiao, L. Wang, Z.-H. Li, X. Chen, and L. Yuan, Bound state in a giant atom-modulated resonators system, *npj Quantum Infom.* **8**, 80 (2022).
- [17] D. D. Noachtar, J. Knörzer, R. H. Jonsson, Nonperturbative treatment of giant atoms using chain transformations, *Phys. Rev. A* **106**, 013702 (2022).
- [18] K. H. Lim, W.-K. Mok, and L.-C. Kwek, Oscillating bound states in non-Markovian photonic lattices, *Phys. Rev. A* **107**, 023716 (2023).
- [19] M. V. Gustafsson, T. Aref, A. F. Kockum, M. K. Ekström, G. Johansson, and P. Delsing, Propagating phonons coupled to an artificial atom, *Science* **346**, 207 (2014).
- [20] A. M. Vadiraj, Andreas Ask, T. G. McConkey, I. Nsanzeza, C. W. Sandbo Chang, A. F. Kockum, and C. M. Wilson, Engineering the level structure of a giant artificial atom in waveguide quantum electrodynamics, *Phys. Rev. A* **103**, 023710 (2021).
- [21] S. Longhi, Photonic simulation of giant atom decay, *Opt. Lett.* **45**, 3017-3020 (2020).
- [22] A. González-Tudela, C. Sánchez Muñoz, and J. I. Cirac, Engineering and Harnessing Giant Atoms in High-Dimensional Baths: A Proposal for Implementation with Cold Atoms, *Phys. Rev. Lett.* **122**, 203603 (2019).
- [23] L. Du, Y. Zhang, J.-H. Wu, A. F. Kockum, and Y. Li, Giant Atoms in Synthetic Frequency Dimensions, *Phys. Rev. Lett.* **128**, 223602 (2022).
- [24] Z. Q. Wang, Y. P. Wang, J. Yao, R. C. Shen, W. J. Wu, J. Qian, J. Li, S. Y. Zhu, and J. Q. You, Giant spin ensembles in waveguide magnonics, *Nat. Commun.* **13**, 7580 (2022).

- [25] M. Saffman, T. G. Walker, and K. Mølmer, Quantum Information with Rydberg Atoms, *Rev. Mod. Phys.* **82**, 2313 (2010).
- [26] D. Møller, L. B. Madsen, and K. Mølmer, Quantum Gates and Multipartite Entanglement by Rydberg Excitation Blockade and Adiabatic Passage, *Phys. Rev. Lett.* **100**, 170504 (2008).
- [27] D. Tiarks, S. Schmidt-Eberle, T. Stolz, G. Rempe, and S. Dürr, A Photon-Photon Quantum Gate Based on Rydberg Interactions, *Nat. Phys.* **15**, 124 (2019).
- [28] M. Khazali and K. Mølmer, Fast Multiqubit Gates by Adiabatic Evolution in Interacting Excited-State Manifolds of Rydberg Atoms and Superconducting Circuits, *Phys. Rev. X* **10**, 021054 (2020).
- [29] K. McDonnell, L. F. Keary, and J. D. Pritchard, Demonstration of a Quantum Gate using Electromagnetically Induced Transparency, *Phys. Rev. Lett.* **129**, 200501 (2022).
- [30] D. Petrosyan and K. Mølmer, Deterministic Free-Space Source of Single Photons Using Rydberg Atoms, *Phys. Rev. Lett.* **121**, 123605 (2018).
- [31] F. Ripka, H. Kübler, R. Löw, T. Pfau, A room-temperature single-photon source based on strongly interacting Rydberg atoms, *Science* **362**, 446 (2018).
- [32] D. P. Ornelas-Huerta, A. N. Craddock, E. A. Goldschmidt, A. J. Hachtel, Y. Wang, P. Bienias, A. V. Gorshkov, S. L. Rolston, and J. V. Porto, On-demand indistinguishable single photons from an efficient and pure source based on a Rydberg ensemble, *Optica* **7**, 813 (2020).
- [33] S. Shi, B. Xu, K. Zhang, G.-S. Ye, D.-S. Xiang, Y. Liu, J. Wang, D. Su, and L. Li, High-fidelity photonic quantum logic gate based on near-optimal Rydberg single-photon source, *Nat. Commun.* **13**, 4454 (2022).
- [34] D. D. Bhaktavatsala Rao and K. Mølmer, Dark Entangled Steady States of Interacting Rydberg Atoms, *Phys. Rev. Lett.* **111**, 033606 (2013).
- [35] H. Levine, A. Keesling, A. Omran, H. Bernien, S. Schwartz, A. S. Zibrov, M. Endres, M. Greiner, V. Vuletić, and M. D. Lukin, High-Fidelity Control and Entanglement of Rydberg-Atom Qubits, *Phys. Rev. Lett.* **121**, 123603 (2018).
- [36] I. S. Madjarov, J. P. Covey, A. L. Shaw, J. Choi, A. Kale, A. Cooper, H. Pichler, V. Schkolnik, J. R. Williams, and M. Endres, High-fidelity entanglement and detection of alkaline-earth Rydberg atoms, *Nat. Phys.* **16**, 857 (2020).
- [37] P.-F. Sun, Y. Yu, Z.-Y. An, J. Li, C.-W. Yang, X.-H. Bao, and J.-W. Pan, Deterministic time-bin entanglement between a single photon and an atomic ensemble, *Phys. Rev. Lett.* **128**, 060502 (2022).
- [38] K. S. Rajasree, T. Ray, K. Karlsson, J. L. Everett, and S. N. Chormaic, Generation of cold Rydberg atoms at submicron distances from an optical nanofiber, *Phys. Rev. Res.* **2**, 012038 (2020).
- [39] Y. Chougale, J. Talukdar, T. Ramos, and R. Nath, Dynamics of Rydberg excitations and quantum correlations in an atomic array coupled to a photonic crystal waveguide, *Phys. Rev. A* **102**, 022816 (2020).
- [40] S. D. Hogan, J. A. Agner, F. Merkt, T. Thiele, S. Filipp, and A. Wallraff, Driving Rydberg-Rydberg Transitions from a Coplanar Microwave Waveguide, *Phys. Rev. Lett.* **108**, 063004 (2012).
- [41] J. S. Douglas, H. H. Habibian, C.-L. Hung, A. V. Gorshkov, H. J. Kimble, and D. E. Chang, Quantum Many-Body Models with Cold Atoms Coupled to Photonic Crystals, *Nat. Photonics* **9**, 326 (2015).
- [42] J. D. Hood, A. Goban, A. Asenjo-Garcia, M. Lu, S.-P. Yu, D. E. Chang, and H. J. Kimble, Atom-atom interactions around the band edge of a photonic crystal waveguide, *Proc. Natl. Acad. Sci. U.S.A.* **113**, 10507 (2016).
- [43] See Supplemental Material at XXX for details, which includes Refs. [44, 45].
- [44] S. Longhi, Quantum decay and amplification in a non-Hermitian unstable continuum, *Phys. Rev. A* **93**, 062129 (2016).
- [45] D. F. James and J. Jerke, Effective Hamiltonian theory and its applications in quantum information, *Can. J. Phys.* **85**, 625-632 (2007).
- [46] H. Breuer and F. Petruccione, *The Theory of Open Quantum Systems* (Oxford University Press, Oxford, 2002).
- [47] G. Calajó, F. Ciccarello, D. Chang, and P. Rabl, Atom-field dressed states in slow-light waveguide QED, *Phys. Rev. A* **93**, 033833 (2016).
- [48] E. Brion, L. H. Pedersen and K. Mølmer, Adiabatic elimination in a lambda system, *J. Phys. A: Math. Theor.* **40**, 1033-1043 (2007).
- [49] D. Yan, J.-W. Gao, Q.-Q. Bao, H. Yang, H. Wang, and J.-H. Wu, Electromagnetically induced transparency in a five-level  $\Lambda$  system dominated by two-photon resonant transitions, *Phys. Rev. A* **83**, 033830 (2011).
- [50] I. I. Beterov, I. I. Ryabtsev, D. B. Tretyakov, and V. M. Entin, Quasiclassical calculations of blackbody-radiation-induced depopulation rates and effective lifetimes of Rydberg nS, nP, and nD alkali-metal atoms with  $n \leq 80$ , *Phys. Rev. A* **79**, 052504 (2009).
- [51] N. Šibalić, J. D. Pritchard, C. S. Adams, and K. J. Weatherill, An introduction to Rydberg atoms with ARC, available online at <https://arc-alkali-rydberg-calculator.readthedocs.io/en/latest/Rydberg-atoms-a-primer-notebook.html>.
- [52] William K. Wootters, Entanglement of Formation of an Arbitrary State of Two Qubits, *Phys. Rev. Lett.* **80**, 2245 (1998).
- [53] K. M. O'connor and W. K. Wootters, Entangled rings, *Phys. Rev. A* **63**, 052302 (2001).
- [54] A. C. Santos and R. Bachelard, Generation of Maximally Entangled Long-Lived States with Giant Atoms in a Waveguide, *Phys. Rev. Lett.* **130**, 053601 (2023).
- [55] J. von Zanthier, T. Bastin, and G. S. Agarwal, Measurement-induced spatial modulation of spontaneous decay and photon arrival times, *Phys. Rev. A* **74**, 061802(R) (2006).
- [56] J. Gillet, G. S. Agarwal, and T. Bastin, Tunable entanglement, antibunching, and saturation effects in dipole blockade, *Phys. Rev. A* **81**, 013837 (2010).
- [57] T. E. Lee, H. Häffner, and M. C. Cross, Collective Quantum Jumps of Rydberg Atoms, *Phys. Rev. Lett.* **108**, 023602 (2012).

# Supplemental Material for “Giant-Atom Effects on Population and Entanglement Dynamics of Rydberg Atoms”

Yao-Tong Chen<sup>1</sup>, Lei Du<sup>1,\*</sup>, Yan Zhang<sup>1</sup>, Lingzhen Guo<sup>2</sup>, Jin-Hui Wu<sup>1,†</sup>, M. Artoni<sup>3,4</sup>, and G. C. La Rocca<sup>5</sup>

<sup>1</sup> School of Physics and Center for Quantum Sciences, Northeast Normal University, Changchun 130024, China

<sup>2</sup> Center for Joint Quantum Studies and Department of Physics, School of Science, Tianjin University, Tianjin 300072, China

<sup>3</sup> Department of Chemistry and Physics of Materials, University of Brescia, Italy

<sup>4</sup> European Laboratory for Non-Linear Spectroscopy, Sesto Fiorentino, Italy

<sup>5</sup> NEST, Scuola Normale Superiore, Piazza dei Cavalieri 7, I-56126 Pisa, Italy

This supplementary material gives further details on the misaligned arrangement of two atoms along a waveguide (Sec. I), the master equation of a two-atom four-level configuration (Sec. II), the master equation of a giant-atom two-level configuration (Sec. III), and the continuous couplings of Rydberg atoms and waveguide modes (Sec. IV) that are omitted in the main text.

## I. MISALIGNED ARRANGEMENT OF TWO ATOMS ALONG A WAVEGUIDE

In this section, we discuss how to manipulate the van der Waals (vdW) potential  $V_6$  and the accumulated phase  $\phi$  separately. As mentioned in the main text,  $V_6$  and  $\phi$  are determined by the (straight-line) distance  $R$  between a pair of Rydberg atoms and the separation  $d$  (along the waveguide) between two coupling points, respectively. When this atomic pair is placed exactly along the waveguide, we have  $R \equiv d$  so that  $\phi$  or  $V_6$  cannot be changed alone as shown in Fig. S1(a). In this case, it is easy to attain  $\phi \simeq \omega_e d / v_g = \omega_e R / v_g = 41.6\pi$  with  $R \simeq 3.1 \mu\text{m}$ ,  $\omega_e \simeq 2\pi \times 1009 \text{ THz}$ , and  $v_g \simeq 0.5c$  as considered in the main text. In order to change  $\phi$  and  $V_6$  separately, we can choose a *misaligned* arrangement of this atomic pair as shown in Fig. S1(b), where  $d$  is clearly smaller than  $R$ . In this case, keeping  $R \simeq 3.1 \mu\text{m}$  and hence  $V_6 = 20 \text{ GHz}$  unchanged, it is viable to tune  $\phi$  in the range of  $[41.6, 39.6]\pi$  by reducing  $d$  from  $3.1 \mu\text{m}$  with a vanishing misaligned angle to  $2.95 \mu\text{m}$  with a  $0.09\pi$  misaligned angle.

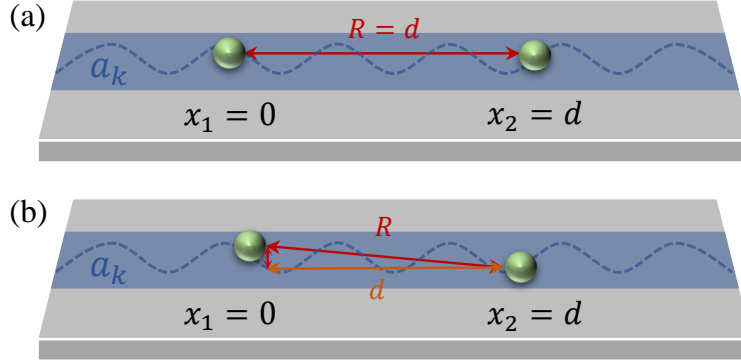


FIG. S1. Arrangement details of two Rydberg atoms with respect to a one-dimensional waveguide shown as a blue area. The atomic pair is (a) placed along the waveguide with  $d = R$ ; (b) misaligned along the waveguide with  $d < R$ .

## II. MASTER EQUATION OF A TWO-ATOM FOUR-LEVEL CONFIGURATION

In this section, we provide the derivation procedures from Eq. (1) on Hamiltonian  $H$  to Eq. (2) on density operator  $\rho$  in the main text. As shown in Fig 1(b), two upper transitions  $|g_1 r_2\rangle \leftrightarrow |r_1 r_2\rangle$  and  $|r_1 g_2\rangle \leftrightarrow |r_1 r_2\rangle$  are driven by the external coherent field  $\Omega_c$  while two lower transitions  $|g_1 g_2\rangle \leftrightarrow |g_1 r_2\rangle$  and  $|g_1 g_2\rangle \leftrightarrow |r_1 g_2\rangle$  are coupled to the waveguide modes. Under the two-photon resonance condition (i.e.,  $\Delta_c \simeq -\delta_k$  with  $\Delta_c = \omega_c - \omega_e - V_6$  and  $\delta_k = \omega_k - \omega_e$ ), we neglect the interactions resulted from coherent field  $\omega_c$  in  $H$  for the moment and move to the interaction picture with

respect to  $H_0 = (2\omega_e + V_6 - \omega_c)(\sigma_+^1\sigma_-^1 + \sigma_+^2\sigma_-^2) + \int dk\omega_k a_k^\dagger a_k = (\omega_e - \Delta_c)(\sigma_+^1\sigma_-^1 + \sigma_+^2\sigma_-^2) + \int dk\omega_k a_k^\dagger a_k$ . Then the Hamiltonian describing the atom-waveguide interaction can be written as

$$\begin{aligned} H_{\text{int}}(t) &= \int_{-\infty}^{+\infty} dk \left[ ge^{-i(\Delta_c + \omega_k - \omega_e)t} a_k \sigma_+^1 + ge^{ikd} e^{-i(\Delta_c + \omega_k - \omega_e)t} a_k \sigma_+^2 + \text{H.c.} \right] \\ &= \int_{-\infty}^{+\infty} dk \left[ ge^{-i(\Delta_c + \delta_k)t} a_k \sigma_+^1 + ge^{ikd} e^{-i(\Delta_c + \delta_k)t} a_k \sigma_+^2 + \text{H.c.} \right] \end{aligned} \quad (\text{S1})$$

with  $\sigma_+^1 = (\sigma_-^1)^\dagger = |r_1 g_2\rangle\langle g_1 g_2|$  and  $\sigma_+^2 = (\sigma_-^2)^\dagger = |g_1 r_2\rangle\langle g_1 g_2|$  defined as in the main text.

To study the population dynamics of this atomic pair, we can eliminate the waveguide field via a standard procedure and calculate the following master equation for a reduced density operator [1, 2]

$$\partial_t \rho(t) = - \int_0^\infty d\tau \text{Tr}_w [H_{\text{int}}(t), [H_{\text{int}}(t - \tau), \rho_w \otimes \rho(t)]], \quad (\text{S2})$$

where  $\text{Tr}_w$  represents a partial tracing over the waveguide degrees of freedom and  $\rho_w = |0\rangle\langle 0|$  is the *initial* vacuum state of the waveguide modes. Substituting Eq. (S1) into Eq. (S2) we have

$$\begin{aligned} \partial_t \rho &= \sum_{j=1,2} \Gamma \left( \sigma_-^j \rho \sigma_+^j - \frac{1}{2} \sigma_+^j \sigma_-^j \rho - \frac{1}{2} \rho \sigma_+^j \sigma_-^j \right) + \frac{\tilde{\Gamma} + \tilde{\Gamma}^*}{2} (\sigma_-^1 \rho \sigma_+^2 + \sigma_-^2 \rho \sigma_+^1) \\ &\quad - \frac{\tilde{\Gamma}}{2} (\sigma_+^1 \sigma_-^2 \rho + \sigma_+^2 \sigma_-^1 \rho) - \frac{\tilde{\Gamma}^*}{2} (\rho \sigma_+^1 \sigma_-^2 + \rho \sigma_+^2 \sigma_-^1) \\ &= \sum_{j=1,2} \Gamma \left( \sigma_-^j \rho \sigma_+^j - \frac{1}{2} \sigma_+^j \sigma_-^j \rho - \frac{1}{2} \rho \sigma_+^j \sigma_-^j \right) + \Gamma_{ex} (\sigma_-^1 \rho \sigma_+^2 + \sigma_-^2 \rho \sigma_+^1) \\ &\quad - \frac{\Gamma_{ex}}{2} (\sigma_+^1 \sigma_-^2 \rho + \sigma_+^2 \sigma_-^1 \rho + \rho \sigma_+^1 \sigma_-^2 + \rho \sigma_+^2 \sigma_-^1) - \frac{iJ_{ex}}{2} (\sigma_+^1 \sigma_-^2 \rho + \sigma_+^2 \sigma_-^1 \rho - \rho \sigma_+^1 \sigma_-^2 - \rho \sigma_+^2 \sigma_-^1), \end{aligned} \quad (\text{S3})$$

with

$$\begin{aligned} \Gamma &= 2g^2 \int_0^\infty d\tau \int_{-\infty}^{+\infty} dk e^{\pm i(\Delta_c + \delta_k)\tau} = 2g^2 \int_0^\infty d\tau e^{\pm i\Delta_c \tau} \left( \int_{-\infty}^0 dk e^{\pm i\delta_k \tau} + \int_0^{+\infty} dk e^{\pm i\delta_k \tau} \right) \\ &= \frac{4g^2}{v_g} \int_0^\infty d\tau e^{\pm i\Delta_c \tau} \int_{-\infty}^{+\infty} d\delta_k e^{\pm i\delta_k \tau} = \frac{4g^2}{v_g} \int_0^\infty d\tau e^{\pm i\Delta_c \tau} 2\pi \delta(\tau) = \frac{4\pi g^2}{v_g} = 4\pi g^2 D(k), \\ \tilde{\Gamma} &= 2g^2 \int_0^\infty d\tau \int_{-\infty}^{+\infty} dk e^{-i(\Delta_c + \delta_k)\tau} e^{\pm ikd} \\ &= 2g^2 \int_0^\infty d\tau \left[ \int_{-\infty}^0 dk e^{-i(\Delta_c + \delta_k)\tau} e^{\mp i(\delta_k + \omega_e)d/v_g} + \int_0^{+\infty} dk e^{-i(\Delta_c + \delta_k)\tau} e^{\pm i(\delta_k + \omega_e)d/v_g} \right] \\ &= \frac{2g^2}{v_g} \int_0^\infty d\tau \left[ \int_{-\infty}^{+\infty} d\delta_k e^{-i(\Delta_c + \delta_k)\tau} e^{\mp i(\delta_k + \omega_e)d/v_g} + \int_{-\infty}^{+\infty} d\delta_k e^{-i(\Delta_c + \delta_k)\tau} e^{\pm i(\delta_k + \omega_e)d/v_g} \right] \\ &= \frac{2g^2}{v_g} \left[ e^{i(\omega_e d/v_g - \Delta_c \tau)} \int_0^\infty d\tau 2\pi \delta(\tau - d/v_g) + e^{-i(\omega_e d/v_g + \Delta_c \tau)} \int_0^\infty d\tau 2\pi \delta(\tau + d/v_g) \right] \\ &= \frac{4\pi g^2}{v_g} e^{i(\omega_e - \Delta_c)d/v_g} \simeq \frac{4\pi g^2}{v_g} e^{i\omega_e d/v_g} = \Gamma e^{i\phi}, \end{aligned} \quad (\text{S4})$$

as well as  $\Gamma_{ex} = \text{Re}\{\tilde{\Gamma}\} = \Gamma \cos\phi$  and  $J_{ex} = \text{Im}\{\tilde{\Gamma}\} = \Gamma \sin\phi$ . In the above derivation, we have also considered the  $\delta$  function definition  $\int_{-\infty}^{+\infty} dk e^{\pm ikx} = 2\pi \delta(x)$  and the waveguide mode density  $D(k) = \partial k / \partial \omega_k$  [3–5].

Note that Eq. (S3) just describes the interactions between a continuum of waveguide modes and two lower atomic transitions  $|g_1 g_2\rangle \leftrightarrow |g_1 r_2\rangle$  and  $|g_1 g_2\rangle \leftrightarrow |r_1 g_2\rangle$ . Further taking into account the intrinsic atomic decay toward non-guided modes in the free space as well as the neglected interactions between a coherent field and two upper atomic transitions  $|g_1 r_2\rangle \leftrightarrow |r_1 r_2\rangle$  and  $|r_1 g_2\rangle \leftrightarrow |r_1 r_2\rangle$  in  $H$ , one can easily obtain the master equation (2) in the main text.

This equation, if expanded in the two-atom four-level configuration, will turn out to be

$$\begin{aligned}
\partial_t \rho_{g_1 g_1, g_2 g_2} &= (\gamma + \Gamma) \rho_{r_1 r_1, g_2 g_2} + (\gamma + \Gamma) \rho_{g_1 g_1, r_2 r_2} + \Gamma_{ex} \rho_{r_1 g_1, g_2 r_2} + \Gamma_{ex} \rho_{g_1 r_1, r_2 g_2}, \\
\partial_t \rho_{r_1 r_1, g_2 g_2} &= -(\gamma + \Gamma) \rho_{r_1 r_1, g_2 g_2} + \gamma \rho_{r_1 r_1, r_2 r_2} - \tilde{\Gamma}/2 \rho_{g_1 r_1, r_2 g_2} - \tilde{\Gamma}^*/2 \rho_{r_1 g_1, g_2 r_2} - i(\Omega_c \rho_{r_1 r_1, g_2 r_2} - \Omega_c^* \rho_{r_1 r_1, r_2 g_2}), \\
\partial_t \rho_{g_1 g_1, r_2 r_2} &= -(\gamma + \Gamma) \rho_{g_1 g_1, r_2 r_2} + \gamma \rho_{r_1 r_1, r_2 r_2} - \tilde{\Gamma}/2 \rho_{r_1 g_1, g_2 r_2} - \tilde{\Gamma}^*/2 \rho_{g_1 r_1, r_2 g_2} - i(\Omega_c \rho_{g_1 r_1, r_2 r_2} - \Omega_c^* \rho_{r_1 g_1, r_2 r_2}), \\
\partial_t \rho_{g_1 r_1, g_2 g_2} &= (i\Delta_c - \gamma/2 - \Gamma/2) \rho_{g_1 r_1, g_2 g_2} + \gamma \rho_{g_1 r_1, r_2 r_2} - \tilde{\Gamma}^*/2 \rho_{g_1 g_1, g_2 r_2} - i\Omega_c \rho_{g_1 r_1, g_2 r_2}, \\
\partial_t \rho_{r_1 g_1, g_2 g_2} &= -(i\Delta_c + \gamma/2 + \Gamma/2) \rho_{r_1 g_1, g_2 g_2} + \gamma \rho_{r_1 g_1, r_2 r_2} - \tilde{\Gamma}/2 \rho_{g_1 g_1, r_2 g_2} + i\Omega_c^* \rho_{r_1 g_1, r_2 g_2}, \\
\partial_t \rho_{g_1 g_1, g_2 r_2} &= (i\Delta_c - \gamma/2 - \Gamma/2) \rho_{g_1 g_1, g_2 r_2} + \gamma \rho_{r_1 r_1, g_2 r_2} - \tilde{\Gamma}^*/2 \rho_{g_1 r_1, g_2 g_2} - i\Omega_c \rho_{g_1 r_1, g_2 r_2}, \\
\partial_t \rho_{g_1 r_1, r_2 g_2} &= -(i\Delta_c + \gamma/2 + \Gamma/2) \rho_{g_1 r_1, r_2 g_2} + \gamma \rho_{r_1 r_1, r_2 g_2} - \tilde{\Gamma}/2 \rho_{r_1 g_1, g_2 g_2} + i\Omega_c^* \rho_{r_1 g_1, r_2 g_2}, \\
\partial_t \rho_{r_1 g_1, r_2 g_2} &= -(i\Delta_c + \gamma/2 + \Gamma/2) \rho_{r_1 g_1, r_2 g_2} + \gamma \rho_{r_1 r_1, r_2 g_2} - \tilde{\Gamma}^*/2 \rho_{r_1 g_1, g_2 r_2} + i\Omega_c^* \rho_{r_1 g_1, r_2 g_2}, \\
\partial_t \rho_{g_1 r_1, g_2 r_2} &= -\gamma \rho_{g_1 r_1, g_2 r_2} - i\Omega_c^* (\rho_{g_1 r_1, g_2 g_2} + \rho_{g_1 g_1, g_2 r_2}), \\
\partial_t \rho_{r_1 g_1, r_2 r_2} &= -\gamma \rho_{r_1 g_1, r_2 r_2} + i\Omega_c (\rho_{r_1 g_1, g_2 g_2} + \rho_{g_1 g_1, r_2 g_2}), \\
\partial_t \rho_{r_1 g_1, g_2 r_2} &= -(\gamma + \Gamma) \rho_{r_1 g_1, g_2 r_2} - \tilde{\Gamma}/2 \rho_{g_1 g_1, r_2 r_2} - \tilde{\Gamma}^*/2 \rho_{r_1 r_1, g_2 g_2} - i(\Omega_c \rho_{r_1 g_1, g_2 r_2} - \Omega_c^* \rho_{r_1 g_1, r_2 r_2}), \\
\partial_t \rho_{g_1 r_1, r_2 g_2} &= -(\gamma + \Gamma) \rho_{g_1 r_1, r_2 g_2} - \tilde{\Gamma}^*/2 \rho_{g_1 g_1, r_2 r_2} - \tilde{\Gamma}/2 \rho_{r_1 r_1, g_2 g_2} + i(\Omega_c^* \rho_{r_1 r_1, r_2 g_2} - \Omega_c \rho_{g_1 r_1, r_2 r_2}), \\
\partial_t \rho_{r_1 r_1, g_2 r_2} &= -(i\Delta_c + 3\gamma/2 + \Gamma/2) \rho_{r_1 r_1, g_2 r_2} - \tilde{\Gamma}/2 \rho_{g_1 r_1, r_2 g_2} - i\Omega_c^* (\rho_{r_1 r_1, g_2 g_2} + \rho_{r_1 g_1, g_2 r_2} - \rho_{r_1 r_1, r_2 r_2}), \\
\partial_t \rho_{r_1 r_1, r_2 g_2} &= (i\Delta_c - 3\gamma/2 - \Gamma/2) \rho_{r_1 r_1, r_2 g_2} - \tilde{\Gamma}^*/2 \rho_{r_1 g_1, r_2 r_2} + i\Omega_c (\rho_{r_1 r_1, g_2 g_2} + \rho_{g_1 r_1, r_2 g_2} - \rho_{r_1 r_1, r_2 r_2}), \\
\partial_t \rho_{g_1 r_1, r_2 r_2} &= -(i\Delta_c + 3\gamma/2 + \Gamma/2) \rho_{g_1 r_1, r_2 r_2} - \tilde{\Gamma}/2 \rho_{r_1 r_1, g_2 r_2} - i\Omega_c^* (\rho_{g_1 r_1, r_2 g_2} + \rho_{g_1 g_1, r_2 r_2} - \rho_{r_1 r_1, r_2 r_2}), \\
\partial_t \rho_{r_1 g_1, r_2 r_2} &= (i\Delta_c - 3\gamma/2 - \Gamma/2) \rho_{r_1 g_1, r_2 r_2} - \tilde{\Gamma}^*/2 \rho_{r_1 r_1, r_2 g_2} + i\Omega_c (\rho_{r_1 g_1, g_2 r_2} + \rho_{g_1 g_1, r_2 r_2} - \rho_{r_1 r_1, r_2 r_2}),
\end{aligned} \tag{S5}$$

constrained by  $\rho_{g_1 g_1, g_2 g_2} + \rho_{r_1 r_1, g_2 g_2} + \rho_{g_1 g_1, r_2 r_2} + \rho_{r_1 r_1, r_2 r_2} = 1$ .

As mentioned in the main text, it is helpful to understand the long-time entanglement onset dynamics by replacing single-excitation states  $|g_1 r_2\rangle$  and  $|r_1 g_2\rangle$  with their superpositions  $|\pm\rangle = 1/\sqrt{2}(|r_1 g_2\rangle \pm |g_1 r_2\rangle)$ . Population evolutions in the two symmetric and anti-symmetric states can be calculated from the above equations as

$$\begin{aligned}
\partial_t \rho_{++} &= \frac{1}{2} (\partial_t \rho_{g_1 g_1, r_2 r_2} + \partial_t \rho_{r_1 r_1, g_2 g_2} + \partial_t \rho_{r_1 g_1, g_2 r_2} + \partial_t \rho_{g_1 r_1, r_2 g_2}) \\
&= \frac{1}{2} \left[ (-\gamma - \Gamma - \tilde{\Gamma}^*/2 - \tilde{\Gamma}/2) (\rho_{g_1 g_1, r_2 r_2} + \rho_{r_1 r_1, g_2 g_2} + \rho_{r_1 g_1, g_2 r_2} + \rho_{g_1 r_1, r_2 g_2}) + \gamma \rho_{r_1 r_1, r_2 r_2} \right] \\
&\quad + i(\Omega_c^* \rho_{r_1 r_1, r_2 g_2} + \Omega_c^* \rho_{r_1 g_1, r_2 r_2} - \Omega_c \rho_{r_1 r_1, g_2 r_2} - \Omega_c \rho_{g_1 r_1, r_2 r_2}) \\
&= -(\gamma + \Gamma + \Gamma_{ex}) \rho_{++} + \gamma \rho_{rr} + i\Omega_c^* \rho_{r+} - i\Omega_c \rho_{+r}, \\
\partial_t \rho_{--} &= \frac{1}{2} (\partial_t \rho_{g_1 g_1, r_2 r_2} + \partial_t \rho_{r_1 r_1, g_2 g_2} - \partial_t \rho_{r_1 g_1, g_2 r_2} - \partial_t \rho_{g_1 r_1, r_2 g_2}) \\
&= \frac{1}{2} \left[ (-\gamma - \Gamma + \tilde{\Gamma}^*/2 + \tilde{\Gamma}/2) (\rho_{g_1 g_1, r_2 r_2} + \rho_{r_1 r_1, g_2 g_2} - \rho_{r_1 g_1, g_2 r_2} - \rho_{g_1 r_1, r_2 g_2}) + \gamma \rho_{r_1 r_1, r_2 r_2} \right] \\
&= -(\gamma + \Gamma - \Gamma_{ex}) \rho_{--} + \gamma \rho_{rr},
\end{aligned} \tag{S6}$$

which are exactly Eq. (8) in the main text if we further introduce  $\gamma_{\pm} = \gamma + \Gamma \pm \Gamma_{ex}$ .

### III. MASTER EQUATION OF A GIANT-ATOM TWO-LEVEL CONFIGURATION

In the case that the single-excitation states  $|r_1 g_2\rangle$  and  $|g_1 r_2\rangle$  are not populated initially, if we have  $|\Delta_c| \gg \Omega_c$ ,  $g$  and  $\Delta_c + \delta_k \simeq 0$ , our two-atom four-level configuration can be reduced to a (synthetic) giant-atom two-level configuration by eliminating  $|r_1 g_2\rangle$  and  $|g_1 r_2\rangle$  in the *short-time* regime. In view of this, a pair of Rydberg atoms will decay from the double-excitation state  $|r_1 r_2\rangle$  directly to the ground state  $|g_1 g_2\rangle$  by simultaneously emitting a coherent-field photon of frequency  $\omega_c$  and a waveguide-mode photon of frequency  $\omega_k$ , through two competing two-photon resonant transitions exhibiting effective coupling strengths  $\xi_1 = -g\Omega_c/\Delta_c \equiv \xi$  and  $\xi_2 = \xi e^{i\phi}$ , respectively. This can be substantiated by the following discussions starting from an *effective* Hamiltonian defined as [6, 7]

$$H_e(t) = -iH_I(t) \int_0^t H_I(t') dt', \tag{S7}$$

with

$$H_I(t) = \int dk g a_k e^{-i(\Delta_c + \delta_k)t} (\sigma_+^1 + e^{ikd} \sigma_+^2) + \Omega_c (\sigma_+^3 + \sigma_+^4) + \text{H.c.} \quad (\text{S8})$$

being the total interaction Hamiltonian involving both waveguide modes and coherent field of our two-atom four-level configuration. Substituting Eq. (S8) into Eq. (S7), one has

$$\begin{aligned} H_e(t) &\simeq \frac{g^2}{\delta_k} \int dk a_k a_k^\dagger (\sigma_-^1 \sigma_+^1 + \sigma_-^2 \sigma_+^2) - \frac{\Omega_c^2}{\Delta_c} (\sigma_+^3 \sigma_-^3 + \sigma_+^4 \sigma_-^4) \\ &\quad + \frac{g\Omega_c}{\delta_k} \int dk a_k e^{-i(\delta_k + \Delta_c)t} (\sigma_+^3 \sigma_+^1 + e^{ikd} \sigma_+^4 \sigma_+^2) - \frac{g\Omega_c}{\Delta_c} \int dk a_k^\dagger e^{i(\delta_k + \Delta_c)t} (\sigma_-^1 \sigma_-^3 + e^{-ikd} \sigma_-^2 \sigma_-^4) + \dots \\ &= \frac{2g^2}{\delta_k} \int dk a_k a_k^\dagger |g_1 g_2\rangle \langle g_1 g_2| - \frac{2\Omega_c^2}{\Delta_c} |r_1 r_2\rangle \langle r_1 r_2| \\ &\quad + \frac{g\Omega_c}{\delta_k} \int dk a_k e^{-i(\delta_k + \Delta_c)t} (1 + e^{ikd}) |r_1 r_2\rangle \langle g_1 g_2| - \frac{g\Omega_c}{\Delta_c} \int dk a_k^\dagger e^{i(\delta_k + \Delta_c)t} (1 + e^{-ikd}) |g_1 g_2\rangle \langle r_1 r_2| + \dots, \end{aligned} \quad (\text{S9})$$

where we have omitted a few terms related to the single-excited states  $|r_1 g_2\rangle$  and  $|g_1 r_2\rangle$  since they are decoupled from other states and only interact with each other.

Considering again  $\Delta_c + \delta_k \simeq 0$  and  $|\Delta_c| \gg \Omega_c, g$  as mentioned above, we have  $|g^2/\delta_k| \rightarrow 0$  and  $|\Omega_c^2/\Delta_c| \rightarrow 0$ , which then result in a reduction of  $H_e$  into the interaction Hamiltonian

$$\mathcal{H}_{\text{int}}(t) = \int_{-\infty}^{+\infty} dk \left[ \xi (1 + e^{ikd}) e^{-i(\delta_k + \Delta_c)t} a_k \sigma_+ + \text{H.c.} \right], \quad (\text{S10})$$

for a synthetic giant atom with two levels  $|g\rangle = |g_1 g_2\rangle$  and  $|r\rangle = |r_1 r_2\rangle$  by taking  $\xi = g\Omega_c/\delta_k = -g\Omega_c/\Delta_c$ . We can attain  $\mathcal{H}$  in Eq. (4) of the main text by rotating this interaction Hamiltonian with respect to frequency  $2\omega_e + V_6$  of the giant-atom transition  $|g\rangle \leftrightarrow |r\rangle$ , which is coupled to a continuum of waveguide modes of frequency  $\omega_k$  accompanied by a coherent field of frequency  $\omega_c$ . Substituting Eq. (S10) into an equation similar to Eq. (S2) for the giant-atom density operator  $\varrho$ , we can further attain the master equation (5) in the main text by including also the intrinsic atomic decay toward non-guided modes in the free space. This master equation turns out to be

$$\begin{aligned} \partial_t \varrho_{gg} &= (\Upsilon + \Upsilon^* + 2\gamma) \varrho_{rr}, \\ \partial_t \varrho_{gr} &= -(\Upsilon^* + \gamma) \varrho_{gr}, \\ \partial_t \varrho_{rg} &= -(\Upsilon + \gamma) \varrho_{rg}, \end{aligned} \quad (\text{S11})$$

after an expansion in the giant-atom two-level configuration and are constrained by  $\varrho_{gg} + \varrho_{rr} = 1$  with

$$\begin{aligned} \Upsilon &= 2\xi^2 \int_0^\infty d\tau \int_{-\infty}^{+\infty} dk \left[ e^{\pm i(\delta_k + \Delta_c)\tau} + e^{-i(\delta_k + \Delta_c)\tau} e^{\pm ikd} \right] \\ &= 4\pi\xi^2 D(k) [1 + e^{i\phi}] = (\Gamma + \Gamma_{ex} + iJ_{ex}) \Omega_c^2 / \Delta_c^2. \end{aligned} \quad (\text{S12})$$

#### IV. CONTINUOUS COUPLINGS OF RYDBERG ATOMS AND WAVEGUIDE MODES

In this section, we try to derive the explicit expressions of relevant constants describing various interactions between two Rydberg atoms and a continuum of waveguide modes modified in the case of continuous couplings. As shown in Fig. 4(a) in the main text, the two continuous couplings around  $x_1 = 0$  and  $x_2 = d$  exhibit a common characteristic width  $\Theta$ , with which relevant exponential distribution functions can be expressed as  $\nu_1(\varphi) = \frac{\sqrt{\Gamma}}{\Theta} e^{-\frac{2}{\Theta}|\varphi|}$  and  $\nu_2(\varphi) = \frac{\sqrt{\Gamma}}{\Theta} e^{-\frac{2}{\Theta}|\varphi - \phi|}$  that satisfy  $\int d\varphi \nu_{1,2}(\varphi) = \sqrt{\Gamma}$  [8]. Here  $\varphi = \phi x/d \simeq \omega_e x/v_g$  describes the phase accumulated from  $x_1$  to  $x$  by a propagating photon along the waveguide and will become  $\phi$  in the case of  $x = x_2$ , which has been considered above for two discrete couplings. In this way, one can immediately generalize the master equation (2) in the main

text to the continuous-coupling case, where the modified constants are given by

$$\begin{aligned}
\Gamma' &= \int_{-\infty}^{\infty} d\varphi \int_{-\infty}^{\infty} d\varphi' \nu_1(\varphi) \nu_1(\varphi') \cos(\varphi - \varphi') \\
&= \frac{\Gamma}{\Theta^2} \int_{-\infty}^{\infty} d\varphi \int_{-\infty}^{\infty} d\varphi' e^{-\frac{2}{\Theta}|\varphi|} e^{-\frac{2}{\Theta}|\varphi'|} \cos(\varphi - \varphi') \\
&= \frac{\Gamma}{\Theta^2} \left[ \int_0^{\infty} d\varphi \int_0^{\infty} d\varphi' e^{-\frac{2}{\Theta}\varphi} e^{-\frac{2}{\Theta}\varphi'} \cos(\varphi - \varphi') + \int_0^{\infty} d\varphi \int_{-\infty}^0 d\varphi' e^{-\frac{2}{\Theta}\varphi} e^{\frac{2}{\Theta}\varphi'} \cos(\varphi - \varphi') \right. \\
&\quad \left. + \int_{-\infty}^0 d\varphi \int_0^{\infty} d\varphi' e^{\frac{2}{\Theta}\varphi} e^{-\frac{2}{\Theta}\varphi'} \cos(\varphi - \varphi') + \int_{-\infty}^0 d\varphi \int_{-\infty}^0 d\varphi' e^{\frac{2}{\Theta}\varphi} e^{\frac{2}{\Theta}\varphi'} \cos(\varphi - \varphi') \right] \\
&= \frac{16\Gamma}{(\Theta^2 + 4)^2},
\end{aligned} \tag{S13}$$

$$\begin{aligned}
J'_{ex} &= \int_{-\infty}^{\infty} d\varphi \int_{-\infty}^{\infty} d\varphi' \nu_1(\varphi) \nu_2(\varphi') \sin|\varphi - \varphi'| \\
&= \frac{\Gamma}{\Theta^2} \int_{-\infty}^{\infty} d\varphi \int_{-\infty}^{\infty} d\varphi' e^{-\frac{2}{\Theta}|\varphi|} e^{-\frac{2}{\Theta}|\varphi' - \phi|} \sin|\varphi - \varphi'| \\
&= \frac{\Gamma}{\Theta^2} \left[ 2 \int_{\phi}^{\infty} d\varphi \int_{\phi}^{\varphi} d\varphi' e^{-\frac{2}{\Theta}\varphi} e^{-\frac{2}{\Theta}(\varphi' - \phi)} \sin(\varphi - \varphi') + \int_{\phi}^{\infty} d\varphi \int_0^{\phi} d\varphi' e^{-\frac{2}{\Theta}\varphi} e^{\frac{2}{\Theta}(\varphi' - \phi)} \sin(\varphi - \varphi') \right. \\
&\quad + \int_{\phi}^{\infty} d\varphi \int_{-\infty}^0 d\varphi' e^{-\frac{2}{\Theta}\varphi} e^{\frac{2}{\Theta}(\varphi' - \phi)} \sin(\varphi - \varphi') + \int_0^{\phi} d\varphi \int_{\phi}^{\infty} d\varphi' e^{-\frac{2}{\Theta}\varphi} e^{-\frac{2}{\Theta}(\varphi' - \phi)} \sin(\varphi - \varphi') \\
&\quad + \int_0^{\phi} d\varphi \int_0^{\varphi} d\varphi' e^{-\frac{2}{\Theta}\varphi} e^{\frac{2}{\Theta}(\varphi' - \phi)} \sin(\varphi - \varphi') + \int_0^{\phi} d\varphi' \int_0^{\varphi'} d\varphi e^{-\frac{2}{\Theta}\varphi} e^{\frac{2}{\Theta}(\varphi' - \phi)} \sin(\varphi' - \varphi) \\
&\quad + \int_0^{\phi} d\varphi \int_{-\infty}^0 d\varphi' e^{-\frac{2}{\Theta}\varphi} e^{\frac{2}{\Theta}(\varphi' - \phi)} \sin(\varphi - \varphi') + \int_{-\infty}^0 d\varphi \int_{\phi}^{\infty} d\varphi' e^{\frac{2}{\Theta}\varphi} e^{-\frac{2}{\Theta}(\varphi' - \phi)} \sin(\varphi' - \varphi) \\
&\quad \left. + \int_{-\infty}^0 d\varphi \int_0^{\phi} d\varphi' e^{\frac{2}{\Theta}\varphi} e^{\frac{2}{\Theta}(\varphi' - \phi)} \sin(\varphi' - \varphi) + 2 \int_{-\infty}^0 d\varphi \int_{-\infty}^{\phi} d\varphi' e^{\frac{2}{\Theta}\varphi} e^{\frac{2}{\Theta}(\varphi' - \phi)} \sin(\varphi - \varphi') \right] \\
&= \frac{\Gamma}{(\Theta^2 + 4)^2} \left[ (8\phi + 2\Theta^2\phi + 12\Theta + \Theta^3) e^{-\frac{2\phi}{\Theta}} + 16\sin\phi \right],
\end{aligned} \tag{S14}$$

$$\begin{aligned}
\Gamma'_{ex} &= \int_{-\infty}^{\infty} \int_{-\infty}^{\infty} d\varphi d\varphi' \nu_1(\varphi) \nu_2(\varphi') \cos(\varphi - \varphi') \\
&= \frac{\Gamma}{\Theta^2} \left[ \int_0^{\infty} d\varphi \int_{\phi}^{\infty} d\varphi' e^{-\frac{2}{\Theta}\varphi} e^{-\frac{2}{\Theta}(\varphi' - \phi)} \cos(\varphi - \varphi') + \int_0^{\infty} d\varphi \int_{-\infty}^{\phi} d\varphi' e^{-\frac{2}{\Theta}\varphi} e^{\frac{2}{\Theta}(\varphi' - \phi)} \cos(\varphi - \varphi') \right. \\
&\quad \left. + \int_{-\infty}^0 d\varphi \int_{\phi}^{\infty} d\varphi' e^{\frac{2}{\Theta}\varphi} e^{-\frac{2}{\Theta}(\varphi' - \phi)} \cos(\varphi - \varphi') + \int_{-\infty}^0 d\varphi \int_{-\infty}^{\phi} d\varphi' e^{\frac{2}{\Theta}\varphi} e^{\frac{2}{\Theta}(\varphi' - \phi)} \cos(\varphi - \varphi') \right] \\
&= \frac{16\Gamma \cos\phi}{(\Theta^2 + 4)^2},
\end{aligned} \tag{S15}$$

with  $\varphi' = \phi x'/v_g$  for a position  $x'$  different from  $x$ . Moreover, an extra coherent interaction term  $\sum_{j=1,2} J' \sigma_+^j \sigma_-^j$  has to be introduced in  $H_{at}$  with the effective interaction strength obtained as

$$\begin{aligned}
J' &= \int_{-\infty}^{\infty} d\varphi \int_{-\infty}^{\infty} d\varphi' \nu_1(\varphi) \nu_1(\varphi') \sin|\varphi - \varphi'| \\
&= \frac{\Gamma}{\Theta^2} \int_{-\infty}^{\infty} d\varphi \int_{-\infty}^{\infty} d\varphi' e^{-\frac{2}{\Theta}|\varphi|} e^{-\frac{2}{\Theta}|\varphi'|} \sin|\varphi - \varphi'| \\
&= \frac{\Gamma}{\Theta^2} \left[ 2 \int_0^{\infty} d\varphi \int_0^{\varphi} d\varphi' e^{-\frac{2}{\Theta}\varphi} e^{-\frac{2}{\Theta}\varphi'} \sin(\varphi - \varphi') + \int_0^{\infty} d\varphi \int_{-\infty}^0 d\varphi' e^{-\frac{2}{\Theta}\varphi} e^{\frac{2}{\Theta}\varphi'} \sin(\varphi - \varphi') \right. \\
&\quad \left. + \int_{-\infty}^0 d\varphi \int_0^{\infty} d\varphi' e^{\frac{2}{\Theta}\varphi} e^{-\frac{2}{\Theta}\varphi'} \sin(\varphi' - \varphi) + 2 \int_{-\infty}^0 d\varphi \int_{-\infty}^{\varphi} d\varphi' e^{\frac{2}{\Theta}\varphi} e^{\frac{2}{\Theta}\varphi'} \sin(\varphi - \varphi') \right] \\
&= \frac{\Gamma\Theta(\Theta^2 + 12)}{(\Theta^2 + 4)^2}.
\end{aligned} \tag{S16}$$

Note also that the expressions of  $J'$  and  $\Gamma'$  will remain unchanged if we replace  $\nu_1$  by  $\nu_2$ , i.e.,

$$\int_{-\infty}^{\infty} d\varphi \int_{-\infty}^{\infty} d\varphi' \nu_1(\varphi) \nu_1(\varphi') e^{i|\varphi - \varphi'|} = \int_{-\infty}^{\infty} d\varphi \int_{-\infty}^{\infty} d\varphi' \nu_2(\varphi) \nu_2(\varphi') e^{i|\varphi - \varphi'|}, \tag{S17}$$

implying that the two constants are identical for both Rydberg atoms.

For the synthetic two-level giant atom, in a similar way,  $\Upsilon = (\Gamma + \Gamma_{ex} + iJ_{ex})\Omega_c^2/\Delta_c^2$  in the case of discrete couplings should be replaced by  $\Upsilon' = (\Gamma' + \Gamma'_{ex} + iJ' + iJ'_{ex})\Omega_c^2/\Delta_c^2$  in the case of continuous couplings.

Finally, we discuss how to control the coupling characteristic width  $\Theta$  in experiment by considering the radial size  $\bar{r}$  of a Rydberg atom. To be more specific, this characteristic width can be estimated as  $\Theta = w\omega_e/v_g = 2\sqrt{\bar{r}^2 - h^2}\omega_e/v_g$  with  $w$  being the overlap width between the electronic distribution of the Rydberg atom and the evanescent field of the waveguide while  $h$  the distance from the Rydberg-atom nucleus to the evanescent-field surface. Then it is viable to attain  $\Theta = 5\pi/2$  with  $h \simeq 449$  nm since we have  $\bar{r} \simeq 583$  nm for  $|r_{1,2}\rangle = |75P_{3/2}\rangle$  [9].

---

\* [dul256@nenu.edu.cn](mailto:dul256@nenu.edu.cn)

† [jhwu@nenu.edu.cn](mailto:jhwu@nenu.edu.cn)

- [1] H. Breuer and F. Petruccione, *The Theory of Open Quantum Systems* (Oxford University Press, Oxford, 2002).
- [2] G. Calajó, F. Ciccarello, D. Chang, and P. Rabl, Atom-field dressed states in slow-light waveguide QED, *Phys. Rev. A* **93**, 033833 (2016).
- [3] A. F. Kockum, P. Delsing, and G. Johansson, Designing frequency-dependent relaxation rates and Lamb shifts for a giant artificial atom, *Phys. Rev. A* **90**, 013837 (2014).
- [4] S. Longhi, Quantum decay and amplification in a non-Hermitian unstable continuum, *Phys. Rev. A* **93**, 062129 (2016).
- [5] B. Kannan, M. Ruckriegel, D. Campbell, A. F. Kockum, J. Braumüller, D. Kim, M. Kjaergaard, P. Krantz, A. Melville, B. M. Niedzielski, A. Vepsäläinen, R. Winik, J. Yoder, F. Nori, T. P. Orlando, S. Gustavsson, and W. D. Oliver, Waveguide quantum electrodynamics with superconducting artificial giant atoms, *Nature (London)* **583**, 775 (2020).
- [6] D. F. James and J. Jerke, Effective Hamiltonian theory and its applications in quantum information, *Can. J. Phys.* **85**, 625-632 (2007).
- [7] D. Yan, J.-W. Gao, Q.-Q. Bao, H. Yang, H. Wang, and J.-H. Wu, Electromagnetically induced transparency in a five-level  $\Lambda$  system dominated by two-photon resonant transitions, *Phys. Rev. A* **83**, 033830 (2011).
- [8] Q. Y. Cai and W. Z. Jia, Coherent single-photon scattering spectra for a giant-atom waveguide-QED system beyond the dipole approximation, *Phys. Rev. A* **104**, 033710 (2021).
- [9] N. Šibalić, J. D. Pritchard, C. S. Adams, and K. J. Weatherill, An introduction to Rydberg atoms with ARC, available online at <https://arc-alkali-rydberg-calculator.readthedocs.io/en/latest/Rydberg-atoms-a-primer-notebook.html>.